ELSEVIER

Ceramics International 33 (2007) 201–205

CERAMICS INTERNATIONAL

www.elsevier.com/locate/ceramint

Increasing the sinterability of tape cast oxalate-derived doped ceria powder by ball milling

Haibin Li, Changrong Xia, Minhui Zhu, Zuoxing Zhou, Xiaoliang Wei, Guangyao Meng *

Department of Materials Science and Engineering, University of Science and Technology of China, Hefei, Anhui 230026, PR China

Received 24 January 2005; received in revised form 2 August 2005; accepted 5 September 2005
Available online 20 December 2005

Abstract

$Ce_{0.8}Sm_{0.2}O_{1.9}$ powder for tape casting has been synthesized by oxalate coprecipitation. The rod-like particles, 1.0 μm sized, were broken to 0.62 μm or 0.37 μm equiaxial particles by 24 or 48 h wet ball milling. The initial sintering rate of tapes is linear with the reciprocal of particle size. The milled 0.37 μm powder densifies to 98% of the theoretical density after sintering at 1400 °C, while the original rod-like powder only densifies to 76%. The different sinterability is due to different particle size and pore texture. Forty-eight hours wet ball milling is needed to increase the sinterability of oxalate-derived doped ceria powder for tape casting.

Keywords: A. Milling; A. Tape casting; A. Sintering; D. CeO_2

1. Introduction

Ceria doped with rare earth oxides shows much higher oxygen ionic conductivity than yttria-stabilized zirconia [1]; it is a potential electrolyte material for solid oxide fuel cells (SOFCs) operated below 700 °C [2]. In SOFCs, the electrolyte layer must have a dense microstructure to avoid direct reaction between fuels at anode and oxygen at cathode, but doped ceria is difficult to densify because of the high melting point (2400 °C) of pure CeO_2. One thousand and six hundred degrees celsius or higher temperature is needed to densify doped ceria synthesized by solid-state reaction [3]. Lower sintering temperature between 1400 and 1500 °C, however, is feasible for doped ceria synthesized by oxalate coprecipitation method [4,5].

Oxalate-derived doped ceria powder is submicron-sized and rod-like. Dry-pressing forming can break the particles into smaller equiaxial ones, and the powder can exhibit high pack density and sinterability. Tape casting forming, frequently used in fabrication of SOFCs [6,7], does not involve a high pressure, and the rod-like powder exhibits poor sinterability: only 70% of the theoretical for tapes sintered at 1400 °C [8]. To break the rod-like particles and increase sinterability, ball milling is involved in tape casting. Some results are summarized in Table 1: the oxalate-derived doped-ceria powders, ball milled by different procedures, show different densities between 70 and 98% of the theoretical after sintering at 1400 °C [8–12].

Dilatometry has been used to analyze the effect of ball milling to sintering dynamics of doped ceria powder [8], but only the compact bodies, not the tape cast ones, have been characterized because of the softness of green tapes from tape casting.

In this work, $Ce_{0.8}Sm_{0.2}O_{1.9}$ powder is synthesized via oxalate coprecipitation; its sinterability is improved by ball milling. The sintering behavior of tapes formed by tape casting is investigated from room temperature to 1400 °C based on density and microstructure evolution.

2. Experimental procedure

Oxalate coprecipitation of $Ce_{0.8}Sm_{0.2}O_{1.9}$ powder begins with the nitrates. Cerium nitrate and samarium nitrate was dissolved in distilled water at a molar ratio of Ce^{3+}:Sm^{3+} = 4:1 to form 1.0 mol L^{-1} solution; then the solution was dropped into 0.05 mol L^{-1} ammonium oxalate solution (pH 6.7) under vigorous stirring to form a white precipitate. The precipitate

* Corresponding author. Tel.: +86 551 3603234; fax: +86 551 3607627.
E-mail addresses: lhb@mail.ustc.edu.cn (H. Li), mgym@ustc.edu.cn (G. Meng).

0272-8842/$32.00
doi:10.1016/j.ceramint.2005.09.003

Table 1
Oxalate coprecipitated doped ceria powders shaped by tape casting and their sinterability

Composition	pH	Pre-heating (°C)	Milling time (h) and medium	Sintering	Relative density (%)	Reference
$Ce_{0.8}Y_{0.2}O_{1.9}$	6.5	800	0	1400 °C, 2 h	<70	[8]
			12–24 (in isopropanol)	1400 °C, 2 h	85	
			12–24 (dry)	1400 °C, 2 h	98	
$Ce_{0.8}Y_{0.2}O_{1.9}$	6.5	600	72 (dry)	1400 °C, 2 h	98	[9]
$Ce_{0.9}Gd_{0.1}O_{1.95}$	6.5	–	6 (in water)	1400 °C, 5 h	93	[10]
$Ce_{0.9}Gd_{0.1}O_{1.95}$	6.5	750	6 (in water)	1400 °C, 5 h	89	[11]
$Ce_{0.8}Sm_{0.2}O_{1.9}$	6.7	600	48 (in ethanol)	1400 °C, 5 h	98	[12]

was filtered, washed, and dried; at last, it was calcined at 350–800 °C for 2 h to form a yellow oxide.

The thermal decomposition of oxalate coprecipitate was analyzed by DTA/TG (Netzsch, STA 429) at a heating rate of 5 °C min^{-1} in air. Phase identification of calcined powders was performed by X-ray diffraction (Philips X' Pert PRO SUPER). The powder morphology was observed by transmission electron microscopy (TEM, H800, Hitachi), and the particle size distribution was measured by a laser particle size analyser (ZetaSize, Malvern).

$Ce_{0.8}Sm_{0.2}O_{1.9}$ powder calcined at 600 °C was ball milled with a laboratory tumbling mill, alcohol solvent, zirconia balls, and polyethylene container. It was ball milled for 0, 24, and 48 h, respectively, and the powders were numbered as powders A–C. The powders A–C were formulated into organic-based casting slurries, while the solid loading was 44%. The slurries were tape cast to form green tapes 1 mm thick. Samples, 20 mm × 20 mm, used in sintering investigation were cut out form the tapes after drying at 60 °C.

The sintering behavior of tape A–C was investigated with a fixed heating program: 1 °C min^{-1} below 500 °C, 2 °C min^{-1} from 500 to 1400 °C, at last, soak at 1400 °C for 5 h. To characterize the sintering behavior, different samples, heated to 500, 800, 1000, 1200, or 1400 °C, were taken out from the oven and cooled in air. The samples were very soft before sintering and very brittle after the binder burnt out at 500 °C. An Abbe optical comparator (Carl Zeiss, Jena) measured the volume shrinkage of all samples and densities were calculated from the mass and volume. The theoretical density of $Ce_{0.8}Sm_{0.2}O_{1.9}$ was taken as 7.15 g cm^{-3} [13]. The microstructure of fracture surface was observed by scanning electron microscopy (SEM, X-650, Hitachi).

3. Results and discussion

In Fig. 1, at 302 °C, similar temperature of $Ce_2(C_2O_4)_3$ decomposition (310 °C) [14,15], the oxalate coprecipitate decomposes to the oxide; no $Sm_2(C_2O_4)_3$ is detected. In Fig. 2, the $Ce_{0.8}Sm_{0.2}O_{1.9}$ oxide powder calcined upon 350 °C exhibits a fluorite structure (JCPDS: 75-0158), and no Sm_2O_3 can be detected in XRD experiment. The crystalline size of the powders is calculated by PowderX program according to Scherrer equation: 15 nm for that calcined at 600 °C. In Fig. 3, TEM micrograph shows the rod-like particle to be a hard agglomerate of small plate-like crystallites.

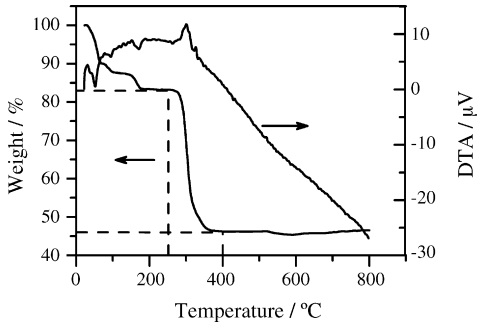

Fig. 1. TG–DTA curve of the coprecipitates.

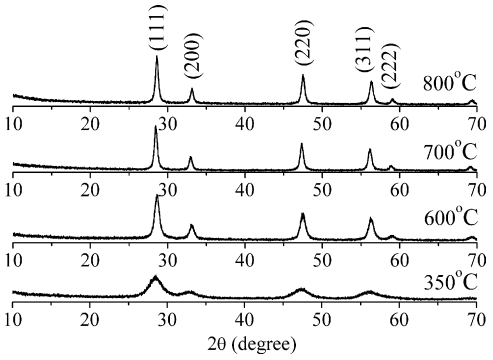

Fig. 2. XRD patterns for $Ce_{0.8}Sm_{0.2}O_{1.9}$ powders calcined at different temperatures.

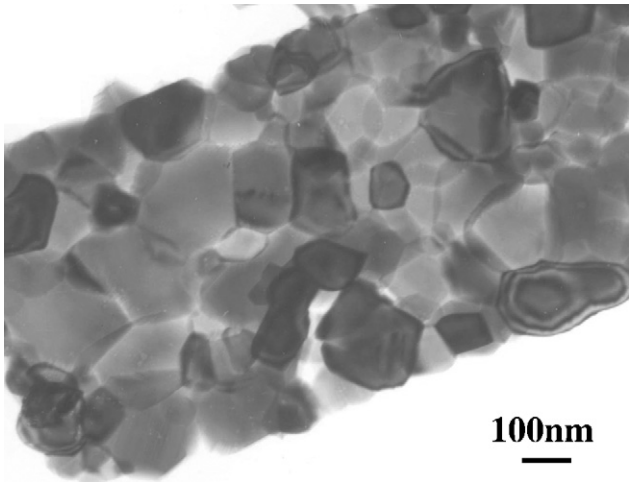

Fig. 3. TEM photo of $Ce_{0.8}Sm_{0.2}O_{1.9}$ particles.

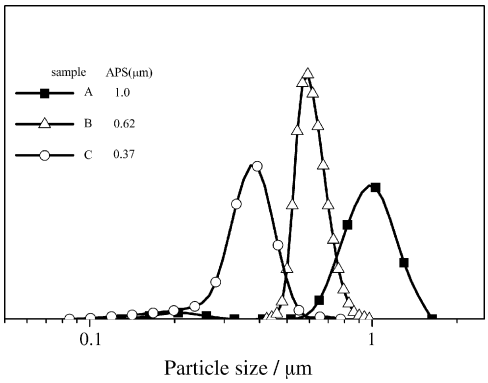

Fig. 4. $Ce_{0.8}Sm_{0.2}O_{1.9}$ particle size distribution after ball milled for different time: (A) 0 h; (B) 24 h; (C) 48 h.

In Fig. 4, the as-calcined powder, A, has an average particle size of 1.0 μm; it reduces to smaller particles with ball milling time: B, 0.62 μm after 24 h milling; C, 0.37 μm after 48 h milling. Fig. 5 shows the sintering behavior of A–C samples: Fig. 5a is the temperature versus time schedule, Fig. 5b is the sintering density versus time. The sintering process is divided into four stages based on the density evolution.

The packing density of powders A–C in green tapes are all about 25% of the theoretical. The densities, however, increase to 26, 31, and 37%, respectively, after organic component burnt out at 500 °C. The microstructure is also different from each other, as shown in Fig. 6. Since the packing density of particles decrease quickly with increasing aspect ratio of them [16], powder A exhibits the lowest packing density, while powder C exhibits the highest.

In Stage II, from 500 to 1000 °C, the densities increase linearly and Eq. (1) describes the sintering rate:

$$v = \frac{\Delta\rho}{\Delta t} = \frac{\rho_2 - \rho_1}{t_2 - t_1}, \tag{1}$$

where $\Delta\rho$ is the increase of density, Δt is the time. The sintering rates of A–C show the ratio:

$$v_A : v_B : v_C = 1 : 1.5 : 2.6, \tag{2}$$

The reciprocal value of particle size of powders A–C show a very similar ratio:

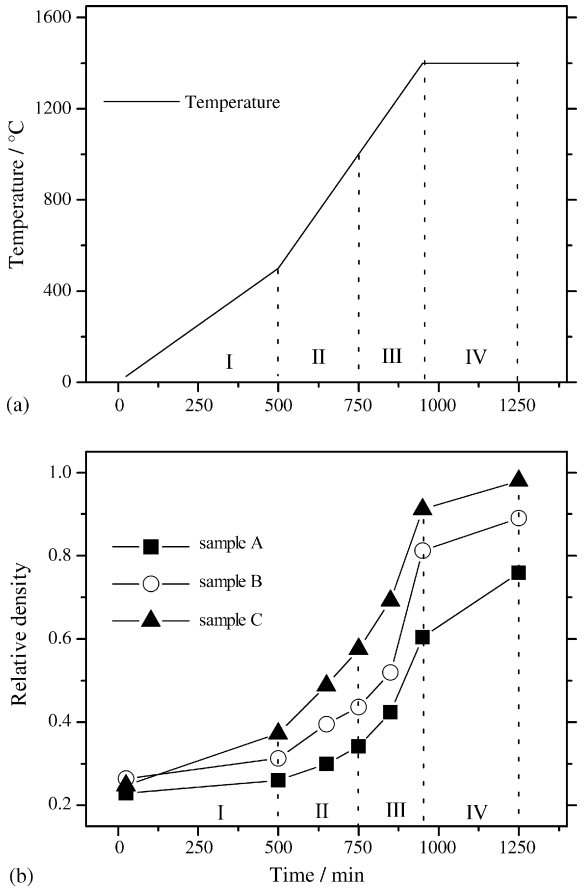

Fig. 5. Relative densities of tapes A–C from room temperature to 1400 °C.

$$\frac{1}{d_A} : \frac{1}{d_B} : \frac{1}{d_C} = 1 : 1.6 : 2.7, \tag{3}$$

where d is the average particle size. Combining formula (2) with formula (3) gives:

$$v_A : v_B : v_C \doteq \frac{1}{d_A} : \frac{1}{d_B} : \frac{1}{d_C}, \tag{4}$$

Sintering shrinkage $\Delta L/L_0$ in the initial stage can be described as [17]:

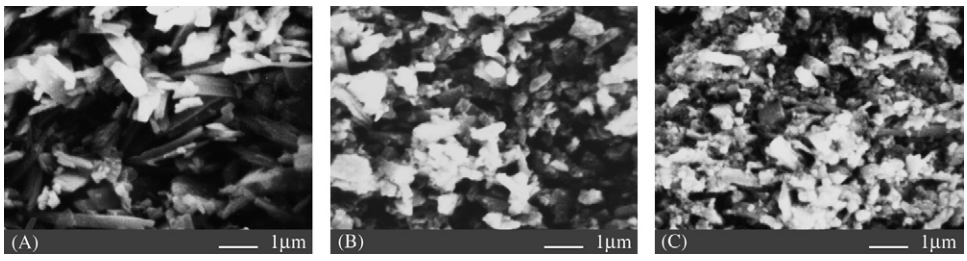

Fig. 6. Package of powders A–C after organic component in the tapes burnt out at 500 °C.

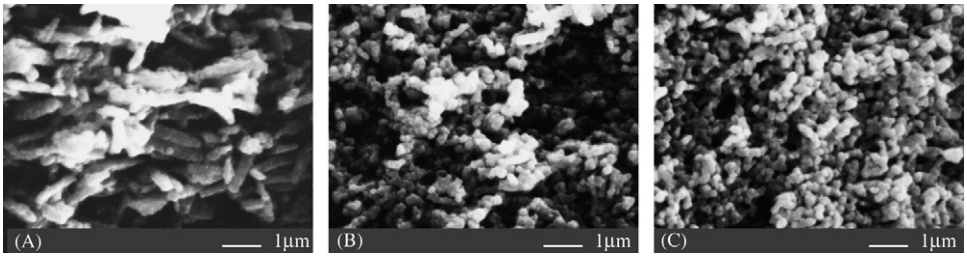

Fig. 7. Microstructure of the tapes A–C heated to 1200 °C.

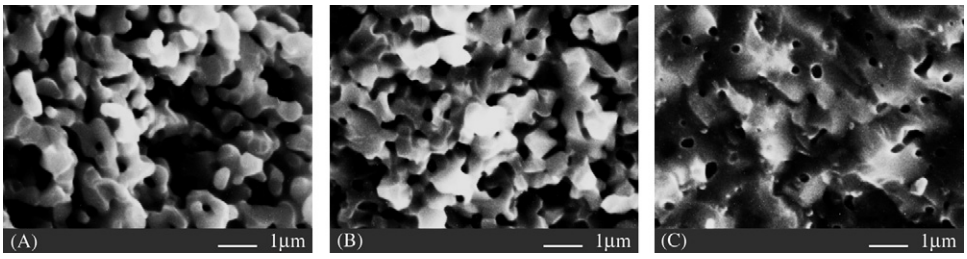

Fig. 8. Microstructure of the tapes A–C heated to 1400 °C.

$$\frac{\Delta L}{L_0} = \left(\frac{KD_V\gamma_S V_V t}{k_B T}\right)^{0.3-0.5} \left(\frac{1}{d}\right)^{\frac{0.3-0.5}{3}}, \quad (5)$$

where d is the grain size. Eq. (5) gives the ratio of sintering rate:

$$\nu_1 : \nu_2 = \left(\frac{1}{d_1}\right)^{0.3-0.5} : \left(\frac{1}{d_2}\right)^{0.3-0.5}. \quad (6)$$

Eqs. (4) and (6) are similar, except the exponent of $1/d$. In our work, after the rod-like powder is ball milled, not only the particle size decreases but also the particle shape, which is essential to sinterability, changes from rod-like to equiaxial. This is probably why the exponent in Eq. (4) is higher than Eq. (6).

In Stage III, the sintering reaches the highest rate in the range of 1200–1400 °C for all three samples despite their different particle size. At 1200 °C, the particles' surfaces become round and smooth (see Fig. 7); at 1400 °C, the grain growth is significant (see Fig. 8). The pore texture, however, is very different from each other. At 1400 °C, pores in A are >1 μm and connected; pores in B are still connected but only about 0.5 μm sized; pores in C are <0.3 μm and closed.

It was pointed out [18] that a pore can be defined by its neighbouring particles, and the number of the particles, N, is defined as the coordination number of the pore. Only pores with small N-value can disappear during the initial stage of sintering; pores with large N-value only can be removed by grain growth at higher temperature or during prolonged heating, after their N decrease enough. In this work, package of A particles forms large, irregular pores with large N-value; the pores are hard to disappear from the sintered body. Package of B or C particles, especially for C, form smaller, more irregular pores with small N-value; the pores are easier to disappear during sintering.

At the end of Stage IV, sintering at 1400 °C for 5 h, densities of A–C reach 76, 89, and 98% of the theoretical, respectively. SEM micrographs are shown in Fig. 9. Only sample C exhibits a dense microstructure, while samples A and B are still porous. It indicates that the oxalate-derived doped ceria powder, formed by tape casting, can be sintered to densify at 1400 °C, only when the particle size is decreased to <0.4 μm by ball milling.

In this work, 24 h wet ball milling only decreases the particle size to 0.62 μm. It means that 24 h wet ball milling is not enough to increase the sinterability of oxalate-derived doped ceria powders formed by tape casting. As shown in Table 1, the oxalate-derived $Ce_{0.8}Y_{0.2}O_{1.9}$ and $Ce_{0.9}Gd_{0.1}O_{1.95}$ powders are also difficult to densify at 1400 °C, when ≤24 h wet ball

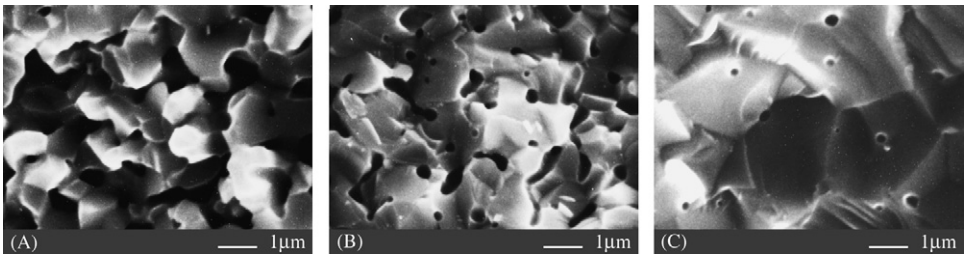

Fig. 9. Microstructure of the tapes A–C after sintered at 1400 °C for 5 h.

milling is used [8,10,11]. The milling time is too short. On the other hand, dry ball milling seems more effective than wet ball milling; 24 h milling has made $Ce_{0.8}Y_{0.2}O_{1.9}$ to densify at 1400 °C [8]. A 72 h dry ball milling [9], however, does not improve the sinterability of $Ce_{0.8}Y_{0.2}O_{1.9}$ much more compared with 24 h dry milling. The above results indicate that 48 h is adequate for wet ball milling, while further milling seems less effective and may cause more pollution from milling media.

4. Conclusions

Oxalate-derived $Ce_{0.8}Sm_{0.2}O_{1.9}$ powder is rod-like; its sinterability in tape casting can be increased by ball milling. Wet ball milling for 24 or 48 h can break the rod-like particles, decrease the particle size from 1 to 0.62 μm, or 0.37 μm. The milled powders show much higher packing density than the unmilled one after burnt out of the organics in green tapes, and the initial sintering rate of tapes, formed by tape casting, is linear with the reciprocal of particle size. All of the three powders, however, show the highest sintering rate in the range of 1200–1400 °C, despite their different particle size. After sintered at 1400 °C for 5 h, only the milled 0.37 μm powder densifies to 98% of the theoretical, while the original rod-like powder only densifies to 76%. Not only the particle size, but also the pore-texture in green tapes influences the sinterability significantly. Forty-eight hours wet ball milling is required to make the oxalate-derived doped ceria, formed by tape casting, densify at 1400 °C, while ≤24 h milling is not enough.

Acknowledgement

This work was supported by the Ministry of Science and Technology of China, under Contract No. 2001AA323090.

References

[1] M. Mogensen, N.M. Sammes, G.A. Tompsett, Physical, chemical and electrochemical properties of pure and doped ceria, Solid State Ionics 129 (1–4) (2000) 63–94.

[2] B.C.H. Steele, Appraisal of $Ce_{1-y}Gd_yO_{2-y/2}$ electrolytes for IT-SOFC operation at 500 °C, Solid State Ionics 129 (1–4) (2000) 95–110.

[3] C.Y. Tian, S.W. Chan, Ionic conductivities, sintering temperatures and microstructures of bulk ceramic CeO_2 doped with Y_2O_3, Solid State Ionics 134 (1/2) (2000) 89–102.

[4] J. VanHerle, T. Horita, T. Kawada, N. Sakai, H. Yokokawa, M. Dokiya, Fabrication and sintering of fine yttria-doped ceria powder, J. Am. Ceram. Soc. 80 (4) (1997) 933–940.

[5] K. Higashi, K. Sonoda, H. Ono, S. Sameshima, Y. Hirata, Synthesis and sintering of rare-earth-doped ceria powder by the oxalate coprecipitation method, J. Mater. Res. 14 (3) (1999) 957–967.

[6] R.J. Gorte, S. Park, J.M. Vohs, C.H. Wang, Anodes for direct oxidation of dry hydrocarbons in a solid-oxide fuel cell, Adv. Mater. 12 (19) (2000) 1465–1469.

[7] A. Mukherjee, B. Maiti, A. Das Sharma, R.N. Basu, H.S. Maiti, Correlation between slurry rheology, green density and sintered density of tape cast yttria stabilised zirconia, Ceram. Int. 27 (7) (2001) 731–739.

[8] J. Van Herle, T. Horita, T. Kawada, N. Sakai, H. Yokokawa, M. Dokiya, Oxalate coprecipitation of doped ceria powder for tape casting, Ceram. Int. 24 (3) (1998) 229–241.

[9] W.S. Jang, S.H. Hyun, S.G. Kim, Preparation of YSZ/YDC and YSZ/GDC composite electrolytes by the tape casting and sol-gel dip-drawing coating method for low-temperature SOFC, J. Mater. Sci. 37 (12) (2002) 2535–2541.

[10] J.G. Cheng, Q.X. Fu, X.Q. Liu, D.K. Peng, G.Y. Meng, Key Engineering Materials, Trans Tech Publications Ltd., Zurich-Uetikon, 2002, pp. 173–177.

[11] J.G. Cheng, S.W. Zha, X.H. Fang, X.Q. Liu, G.Y. Meng, On the green density, sintering behavior and electrical property of tape cast $Ce_{0.9}Gd_{0.1}O_{1.95}$ electrolyte films, Mater. Res. Bull. 37 (15) (2002) 2437–2446.

[12] H.B. Li, C.R. Xia, X.H. Fang, X. He, X.L. Wei, G.Y. Meng, Co-sintering of SDC/NiO-SDC bi-layers prepared by tape casting, Key Eng. Mater. 280–283 (2005) 779–784.

[13] Y.R. Wang, T. Mori, J.-G. Li, Y. Yajima, Low-temperature fabrication and electrical property of 10 mol% Sm_2O_3-doped CeO_2 ceramics, Sci. Technol. Adv. Mater. 4 (2003) 229–238.

[14] W.W. Wendlandt, Thermal decomposition of scandium, yttrium, and rare earth metal oxalates, Anal. Chem. 30 (1) (1958) 58–61.

[15] M.J. Fuller, J. Pindstone, Thermal analysis of the oxalate hexahydrates and decahydrates of yttrium and the lanthanide elements, J. Less-Common Met. 70 (1980) 127–142.

[16] M.N. Rahaman, Ceramic Processing and Sintering, second ed., Marcel Dekker, Inc., New York, 2003.

[17] J.S. Reed, Principles of Ceramics Processing, second ed., John Wiley & Sons, Inc., New York, 1994.

[18] F.F. Lange, Powder processing science and technology for increased reliability, J. Am. Ceram. Soc. 72 (1) (1989) 3–15.